Isomerization pathways from the norbornadiene to the cycloheptatriene radical cation by opening a bridgehead-methylene bond: a theoretical investigation†

Daniel Norberg,[a] Per-Erik Larsson[b] and Nessima Salhi-Benachenhou*[a]

Received 4th September 2006, Accepted 22nd September 2006
First published as an Advance Article on the web 18th October 2006
DOI: 10.1039/b612791f

Three skeletal rearrangement channels for the norbornadiene ($N^{\bullet+}$) to the 1,3,5-cycloheptatriene ($CHT^{\bullet+}$) radical cation conversion, initialized by opening a bridgehead-methylene bond in $N^{\bullet+}$, are investigated using the quantum chemical B3LYP, MP2 and CCSD(T) methods in conjunction with the 6–311+G(d,p) basis set. Two of the isomerizations proceed through the norcaradiene radical cation ($NCD^{\bullet+}$), either through a concerted path ($N^{\bullet+}$ – $NCD^{\bullet+}$), or by a stepwise mechanism *via* a stable intermediate ($N^{\bullet+}$ – I1 – $NCD^{\bullet+}$). At the CCSD(T)/6–311+G(d,p)//B3LYP/6–311+G(d,p) level, the lowest activation energy, 28.9 kcal mol^{-1}, is found for the concerted path whereas the stepwise path is found to be 2.3 kcal mol^{-1} higher. On both pathways, $NCD^{\bullet+}$ rearranges further to $CHT^{\bullet+}$ with significantly less activation energy. The third channel proceeds from $N^{\bullet+}$ through I1 and then directly to $CHT^{\bullet+}$, with an activation energy of 37.1 kcal mol^{-1}. The multi-step channel reported earlier by our group, which proceeds from $N^{\bullet+}$ to $CHT^{\bullet+}$ *via* the quadricyclane and the bicyclo[2.2.1]hepta-2-ene-5-yl-7-ylium radical cations, is 4.6 kcal mol^{-1} lower than the most favorable path of the present study. If the methylene group is substituted with $C(CH_3)_2$, however, the concerted path is estimated to be 5.6 kcal mol^{-1} lower than the corresponding substituted multi-step path at the B3LYP/6–311+(d,p) level. This shows that substitution of particular positions can have dramatic effects on altering reaction barriers in the studied rearrangements. We also note that identical energies are computed for $CHT^{\bullet+}$ and $NCD^{\bullet+}$ whereas, in earlier theoretical investigations, the former was reported to be 6–17 kcal mol^{-1} more stable than the latter. Finally, a bent geometry is obtained for $CHT^{\bullet+}$ with MP2/6–311+G(d,p) in contradiction with the planar conformation reported for this cation in earlier computational studies.

Introduction

Hydrocarbon radical cations with strained ring structures have a tendency to undergo facile rearrangement reactions in order to release their strain energy. Such rearrangements occur with lower barriers than those of the parent neutral molecules, often yielding a variety of unexpected structures on the potential energy surface (PES) of the radical cation.[1]

In particular, the PES of $C_7H_8^{\bullet+}$ has been reported[2] to contain an unusually large number of stable isomers. These include the radical cations of norbornadiene ($N^{\bullet+}$), quadricyclane ($Q^{\bullet+}$), 1,3,5-cycloheptatriene ($CHT^{\bullet+}$), toluene ($T^{\bullet+}$) and 5-methylenecyclohexa-1,3-diene ($MCH^{\bullet+}$) which all have been the focus of many experimental and theoretical investigations. One of the most studied reactions on this surface is the facile isomerization of $Q^{\bullet+}$ to $N^{\bullet+}$, which has become a prototype for one-electron oxidation reactions[3–10] and which has also been given special attention as a potential application for solar energy storage.[11] In parallel, the chemistry of $C_7H_8^{\bullet+}$ was also readily augmented with new rearrangement pathways, allowing for the observation of additional ionic species together with $Q^{\bullet+}$ and $N^{\bullet+}$ when quadricyclane (Q) and norbornadiene (N) are ionized[5,7,12–14] (see Scheme 1). In particular, after ionization of both Q and N, electron spin resonance (ESR) data[5,7,12] indicate the presence of $CHT^{\bullet+}$.

Recently, we have undertaken computational studies[15] for the isomerization reactions of $Q^{\bullet+}$ to the bicyclo[3.2.0]hepta-2,6-diene radical cation ($BHD^{\bullet+}$), as well as for the further rearrangement[16] to $CHT^{\bullet+}$ (see Scheme 1). Using quantum chemical B3LYP, MP2 and CCSD(T) methods,[17] a mechanism was proposed for the skeletal rearrangement of $Q^{\bullet+}$ to $BHD^{\bullet+}$, which was found to occur *via* a stable intermediate, the bicyclo[2.2.1]hepta-2-ene-5-yl-7-ylium radical cation ($BHE^{\bullet+}$). At the CCSD(T)/6–311+G(d,p)//B3LYP/6–311+G(d,p) level of calculation,[17] $BHE^{\bullet+}$ was found to be 2.5 kcal mol^{-1} more stable than $BHD^{\bullet+}$ and, moreover, the barrier of the $Q^{\bullet+}$ to $BHE^{\bullet+}$ reaction was found

[a]*Department of Quantum Chemistry, Uppsala University, Box 518, 751 20, Uppsala, Sweden. E-mail: Nessima.Salhi@kvac.uu.se*
[b]*Department of Chemistry, University of Bath, Bath, United Kingdom BA2 7AY*

† Electronic supplementary information (ESI) available: Total energies and *xyz*-matrices of the B3LYP/6–311+G(d,p), HF/6–311+G(d,p) and MP2/6–311+G(d,p) optimized stationary structures, total CCSD(T)/6–311+G(d,p) energies and thermal corrections to Gibbs free energy at 1.0 atm and 100 K for the $C_7H_8^{\bullet+}$ B3LYP doublet structures, $\langle S^2 \rangle$ values for the MP2 optimized structures and the imaginary frequencies of the TS optimized at all computational levels and the B3LYP/6–311+G(d,p) calculated Mulliken charges, atomic spin densities and ^{1}H hfcc values for the intermediate ion I1. See DOI: 10.1039/b612791f

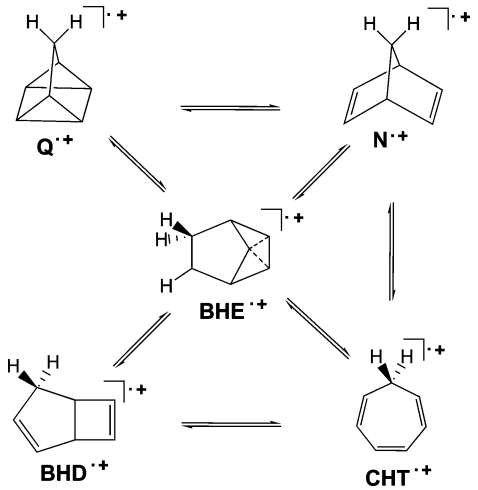

Scheme 1

to be 4.9 kcal mol^{-1} higher than the barrier of the facile Q$^{\bullet+}$ to N$^{\bullet+}$ rearrangement.[15] Also, starting from BHE$^{\bullet+}$, a multistep isomerization pathway leading to the formation of CHT$^{\bullet+}$ was identified. At the above mentioned level of theory, the rate-limiting step on this path has a barrier of 16.5 kcal mol^{-1} above Q$^{\bullet+}$, whereas the barrier was found[16] to be higher (19.3 kcal mol^{-1}) when BHE$^{\bullet+}$ rearranges to CHT$^{\bullet+}$ *via* BHD$^{\bullet+}$. The novel distonic BHE$^{\bullet+}$ intermediate is characterized, moreover, by a homoaromatic stabilization in a three-centre two-electron bond.[18]

In addition, there are other interesting rearrangement channels on the $C_7H_8^{\bullet+}$ PES, such as the path connecting N$^{\bullet+}$ directly to BHE$^{\bullet+}$, which is ~5 kcal mol^{-1} higher than the path connecting N$^{\bullet+}$ to BHE$^{\bullet+}$, *via* Q$^{\bullet+}$, as computed with CCSD(T)/cc-pVDZ//B3LYP/6–31G(d). However, if both N$^{\bullet+}$ and Q$^{\bullet+}$ bear a methylene group on the 7-position (C_1 in Fig. 1), the corresponding substituted paths become competitive.[19] Another case where substitution affects the product outcome is the one-electron oxidation of isopropylidene substituted Q, which gives only isopropylidene substituted BHD as product, in quantitative yield.[20]

On the neutral C_7H_8 PES, Davidson and co-workers[21] investigated the mechanism for the interconversion of CHT and norcaradiene (NCD), also involving toluene (T), using both multi-reference and density functional theory (DFT) methods. The connection of these compounds with N was not explicitly undertaken but a diradical intermediate, first proposed by Woods,[22] was assumed as a shallow intermediate following opening of one of the bridgehead-methylene bonds in N before ring-closure to NCD. To the best of our knowledge the corresponding radical cation rearrangement, leading to CHT$^{\bullet+}$, has not been suggested to be the mechanism for the CHT$^{\bullet+}$ formation. This may suggest a high barrier for the bridgehead-methylene bond cleavage in N$^{\bullet+}$. However, a stabilization or destabilization with particular substituents might induce profound changes in the reaction energetics of radical cations. A recent mass spectral investigation of substituted norbornane β-amino alcohols provides a good example.[23] After ionization of 1-amino-3,3-dimethylnorbornan-2-ols and isomeric 1-amino-7,7-dimethylnorbornan-2-ols the mass-spectral data are dominated in both cases by the cyclopentenylimmonium ion formed by initial C_1–C_2 bond cleavage (C_4–C_5 in our notation, see Fig. 1). However, the latter mass-spectrum is readily augmented

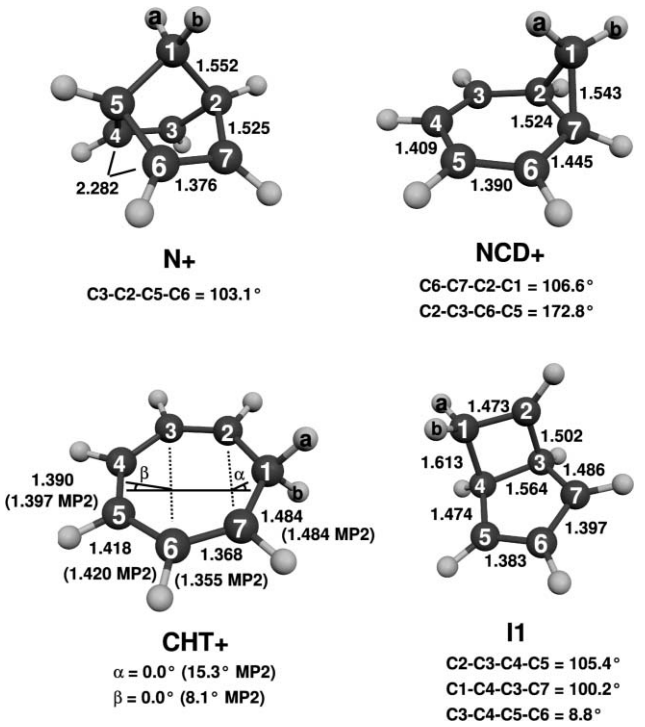

Fig. 1 B3LYP/6–311+G(d,p) optimized geometries of the local minima. The MP2/6–311+G(d,p) geometry of CHT$^{\bullet+}$ is also given for comparison (see text). Bond lengths are given in Ångström.

with additional products originating from initial cleavage of the bridgehead-methylene bond in the parent radical cation. Thus, a relatively minor shift in the substitution pattern can alter the fragmentation pattern and, further, gives strong indication that the breaking of the bridgehead-methylene bond under such conditions can become competitive with the lowest energy path.

Hence, in the present article we report on the results from quantum chemical investigations of three isomerization channels for the transformation of N$^{\bullet+}$ to CHT$^{\bullet+}$, which are all initialized by cleavage of one of the bridgehead-methylene bonds in N$^{\bullet+}$. In particular, two paths which pass through NCD$^{\bullet+}$ as an intermediate following either a concerted or a stepwise process are characterized and compared to the corresponding transformations to neutral NCD. Besides, a novel stable ionic species is identified on the already very rich PES of $C_7H_8^{\bullet+}$ and some features concerning the structure and the relative stability of CHT$^{\bullet+}$ and NCD$^{\bullet+}$ are also presented and compared to the findings of earlier theoretical studies. Finally, by adding two methyl groups at the methylene position, the effects of substitution on the lowest energy path located in this work are investigated.

Computational details

The Gaussian 03 suite of programs has been used for all quantum chemical calculations and the abbreviations relating to the employed methods are taken from this program package.[24] Molekel[25] was used for visual inspection of the final geometries and vibrational frequencies, and for making pictures of the optimized stationary points.

A preliminary investigation of the $C_7H_8^{\bullet+}$ PES was performed using B3LYP/6–31G(d,p) in the unrestricted formalism. At this

level of theory we made sure that stationary points connected correctly to each other in the sense of "minimum-transition structure-minimum" by performing IRC calculations followed by steepest descent optimizations and furthermore, by analyzing the imaginary frequency of the transition structure. The stationary points optimized with B3LYP/6–31G(d,p) were subsequently re-optimized using B3LYP/6–311+G(d,p), which is our production method for the geometries and frequencies in this work. In order to evaluate the reliability of the B3LYP/6–311+G(d,p) structures, the B3LYP/6–31G(d,p) geometries were also optimized using MP2/6–311+G(d,p). However, only HF/6–311+G(d,p) level of calculation has been used for the optimization of two of the transition structures (TS1 and TS3, see below) which could not be obtained at the MP2 level. For the substituted species the geometries and energies have been obtained at the B3LYP/6–311+G(d,p) level. The normal modes of the imaginary frequencies in the substituted transition structures were inspected and it was made sure that they all correspond to the same modes as in the corresponding unsubstituted transition structures. All geometry optimizations were performed without any symmetry constraint and using the default convergence criterions of displacements and forces on the nuclei. Electronic energies for the compounds on the $C_7H_8^{\bullet+}$ PES were calculated at the B3LYP/6–311+G(d,p) geometries using coupled-cluster CCSD(T)/6–311+G(d,p). The convergence criterion on the root mean square of the SCF–density matrix in the CCSD(T) calculations was set to 10^{-10}. Finally, Gibbs energy profiles were constructed by adding the CCSD(T)/6–311+G(d,p) electronic energy with the B3LYP/6–311+G(d,p) thermal correction to Gibbs free energy at 1.0 atm and 100 K (using unscaled vibrational frequencies).

As has been noted before for radical cation systems (see, *e.g.*, ref. 16), the SCF reference wavefunctions for most of the stationary points optimized with MP2/6–311+G(d,p) are found to be heavily spin-contaminated: 0.763 ($N^{\bullet+}$) $\leq \langle S^2 \rangle \leq$ 1.023 ($CHT^{\bullet+}$) for the minima and 0.905 (TS2) $\leq \langle S^2 \rangle \leq$ 1.147 (TS1) for the transition structures. In contrast, for B3LYP the $\langle S^2 \rangle$ values are 0.753–0.765 for the minima and 0.754–0.773 for the transition structures. SCF spin-contamination is a less severe problem in the CCSD(T) calculations since the major spin-contaminant is annihilated from the CCSD wavefunction.[26]

For ease of notation, the abbreviations B3LYP, MP2 and CCSD(T) stand for B3LYP/6–311+G(d,p), MP2/6–311+G(d,p) and CCSD(T)/6–311+G(d,p), respectively. However, when the reaction paths are discussed in terms of IRC and steepest descent calculations, we always refer to the results obtained using the 6–31G(d,p) basis set.

Results and discussion

Three rearrangement channels from $N^{\bullet+}$ to $CHT^{\bullet+}$ are investigated in the present study. All three pathways are initialized by opening of a bridgehead-methylene bond in $N^{\bullet+}$. The first pathway: $N^{\bullet+}$ – TS1 – $NCD^{\bullet+}$ – TS2 – $CHT^{\bullet+}$, proceeds in a single step to $NCD^{\bullet+}$ followed by ring opening to $CHT^{\bullet+}$, whereas the second pathway: $N^{\bullet+}$ – TS3 – I1 – TS4 – $NCD^{\bullet+}$ – TS2 – $CHT^{\bullet+}$, involves a stable intermediate, I1 (see below). The third reaction path proceeds from $N^{\bullet+}$ through I1 and then directly to $CHT^{\bullet+}$: $N^{\bullet+}$ – TS3 – I1 – TS5 – $CHT^{\bullet+}$.

The B3LYP optimized structures of the local minima $N^{\bullet+}$, $NCD^{\bullet+}$, $CHT^{\bullet+}$ and I1 are displayed in Fig. 1 with selected geometrical parameters. The atoms have been labelled in such a way that one can follow the skeletal rearrangement of the lowest energy path from $N^{\bullet+}$ to $CHT^{\bullet+}$ (*i.e.*, $N^{\bullet+}$ – $NCD^{\bullet+}$ – $CHT^{\bullet+}$) in a consistent manner. Table 1 displays the ^{1}H hyperfine coupling constants (hfcc) calculated for these ions at the B3LYP and MP2 levels. As can be seen in the Table, for both $N^{\bullet+}$ and $CHT^{\bullet+}$, the hfcc values computed with B3LYP are in very good agreement with the experimental ones. MP2, on the contrary, fails to predict correctly the hfcc values of $CHT^{\bullet+}$, both qualitatively and quantitatively. We attribute this failure to the very large spin-contamination of the

Table 1 ^{1}H hfcc values (in Gauss) for $N^{\bullet+}$, $NCD^{\bullet+}$, $CHT^{\bullet+}$ and I1, as computed with B3LYP and MP2. See Fig. 1 for the atom labels

Computation method	^{1}H hfcc values							
	$N^{\bullet+}$							
	a_H(1a,1b)	a_H(2,5)	a_H(3,4,6,7)					
B3LYP	4.2	−0.5	−7.2					
MP2	3.0	−0.7	−8.5					
Exp[a]	*3.28*	*0.58*	*7.98*					
	$NCD^{\bullet+}$							
	a_H(1a)	a_H(1b)	a_H(2,7)	a_H(3,6)	a_H(4,5)			
B3LYP	−5.7	−6.2	14.9	−7.5	−2.7			
MP2	−6.0	−9.0	11.6	−4.7	−7.4			
	$CHT^{\bullet+}$							
	a_H(1a)	a_H(1b)	a_H(2,7)	a_H(3,6)	a_H(4,5)			
B3LYP	51.2	51.2	−6.9	−0.7	−4.7			
MP2	56.9	21.4	2.8	−12.3	−4.3			
Exp[b]	*51.5*	*51.5*	*5.7*	—	*5.7*			
	I1							
	a_H(1a)	a_H(1b)	a_H(2)	a_H(3)	a_H(4)	a_H(5)	a_H(6)	a_H(7)
B3LYP	15.2	21.7	−14.9	44.8	6.7	−7.0	0.7	−4.5
MP2	5.4	15.9	−16.7	40.5	3.1	0.2	−8.2	−6.5

[a] ^{1}H hfcc values assigned to an ESR spectrum of $N^{\bullet+}$ in a zeolite matrix at 175 K.[7] [b] ^{1}H hfcc values assigned to an ESR spectrum of $CHT^{\bullet+}$ in a $CF_2ClCFCl_2$ matrix at 77 K.[29]

MP2 reference wave-function for this species ($\langle S^2 \rangle = 1.023$). The fact that MP2 calculates markedly different hfcc values for the two methylene hydrogen atoms in $CHT^{\bullet+}$, $a_H(1a) = 56.9$ G and $a_H(1b) = 21.4$ G (see Fig. 1 for the atom labels), is attributed to the non-planar structure predicted for this ion by MP2, a feature which is discussed below. Hence, the excellent B3LYP hfcc values for $N^{\bullet+}$ and $CHT^{\bullet+}$ give further support for the suggestion[27] that this functional is a good computational choice for calculating hfcc values for organic radicals. While MP2, on the other hand, often predicts highly spin-contaminated structures and therefore much care must be taken when using its results.[28]

Comparing the local minima optimized with B3LYP/6–311+G(d,p) and B3LYP/6–31G(d,p), the largest geometrical deviations are 0.003 Å, 1.3° and 1.0° for bond distances, bond angles and dihedral angles, respectively. B3LYP and MP2 are found to be in quite good agreement for the geometry optimization of $N^{\bullet+}$, $NCD^{\bullet+}$ and I1, the maximum absolute deviations between the two methods being of 0.014 Å (C_2–C_7 in $NCD^{\bullet+}$) for distances, 5.6° (C_2–C_3–C_7 in I1) for bond angles and 5.0° (C_1–C_2–C_3–C_4 in $NCD^{\bullet+}$) for dihedral angles. Both the B3LYP and MP2 optimized structures of $NCD^{\bullet+}$ are found to be essentially in agreement with previous computational predictions of its geometry.[30]

The B3LYP optimized transition structures TS1, TS2, TS3, TS4 and TS5 are displayed in Fig. 2 with selected geometrical parameters. The largest geometrical deviations between the geometry optimized with B3LYP/6–311+G(d,p) and those optimized with B3LYP/6–31G(d,p) are 0.005 Å, 0.7° and 1.1° for bond distances, bond angles and dihedral angles, respectively. The HF optimized structures of TS1 and TS3 are in good agreement with the B3LYP ones, whereas for TS2, TS4 and TS5 the MP2 geometries show larger deviations from the corresponding B3LYP structures. In general, the geometrical parameters involved in the reaction coordinate have the largest differences. For example, for TS3 the largest deviations between B3LYP and HF are found in the parameters related to the opening of one bridgehead-methylene bond (C_1–C_5), $\Delta(C_1$–$C_5) = 0.060$ Å, and the formation of the C_1–C_4 bond, $\Delta(C_1$–$C_4) = 0.064$ Å, where Δ = B3LYP − [HF or MP2]. For TS2, $\Delta(C_2$–$C_7) = -0.137$ Å, $\Delta(C_2$–C_1–$C_7) = -7.5°$ and $\Delta(C_1$–C_2–C_3–$C_4) = -9.9°$ and, compared to MP2, B3LYP predicts an earlier transition structure for the ring opening of $NCD^{\bullet+}$ to $CHT^{\bullet+}$. On the contrary, for the formation of $NCD^{\bullet+}$ from I1, TS4 is predicted to be a later transition structure with B3LYP compared to MP2. The largest deviations between the two methods for TS4 are found to be $\Delta(C_3$–$C_4) = 0.120$ Å, $\Delta(C_2$–C_3–$C_7) = 8.2°$ and $\Delta(C_4$–C_1–C_2–$C_3) = -8.3°$. Finally, with regards to TS5, the two methods are in good agreement, showing only small differences for the coordinates involved in the isomerization from I1 to $CHT^{\bullet+}$ (*e.g.*, $\Delta(C_3$–$C_4) = -0.030$ Å and $\Delta(C_2$–$C_7) = 0.033$ Å).

$CHT^{\bullet+}$

Previous theoretical predictions[16,31] and most of the experimental observations[5,29,32] support a planar C_{2v} structure for $CHT^{\bullet+}$. To our knowledge, only one experimental ESR investigation[33] of this ion, which was performed in a CCl_3CF_3 matrix at 70 K, indicates that the equilibrium geometry might be slightly bent, but much less pronounced than in the neutral compound (see, *e.g.*, ref. 31 and references therein). However, the authors of this experimental work concluded[33] that the observed non-planarity of $CHT^{\bullet+}$ probably reflects matrix effects. In the present study, B3LYP predicts a planar structure for $CHT^{\bullet+}$ with geometrical parameters in good agreement with those reported in the earlier quantum chemical studies.[16,31] However, as mentioned above, a non-planar conformation is found in the MP2/6–311+G(d,p) geometry optimization calculations for $CHT^{\bullet+}$, similar to the bent structure computed[31] for neutral CHT. Nevertheless, the

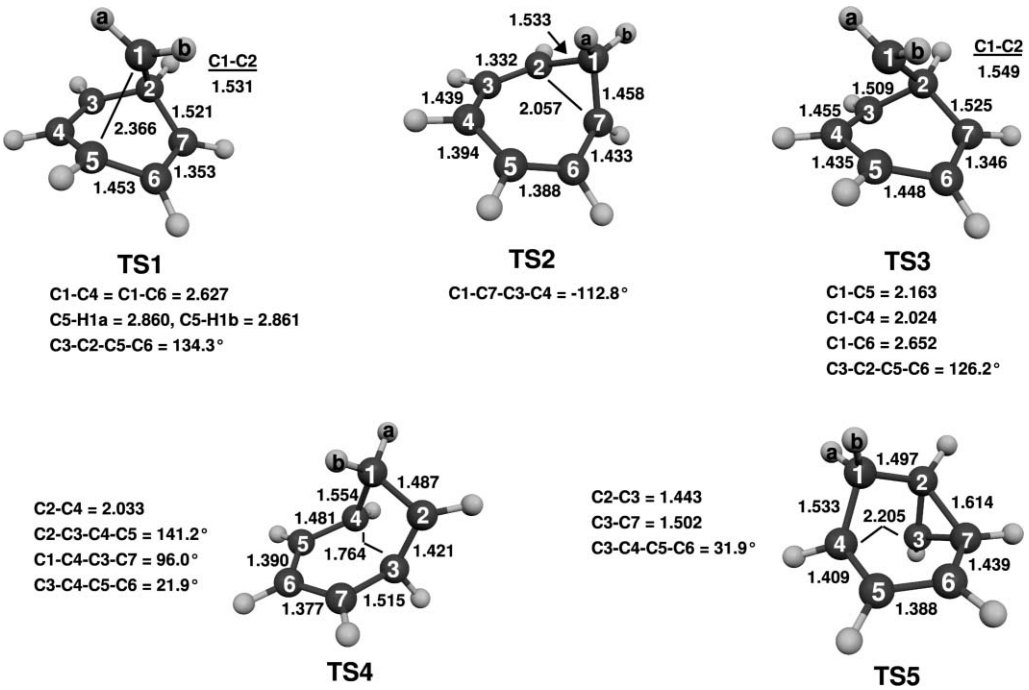

Fig. 2 B3LYP/6–311+G(d,p) optimized geometries of the transition structures. Bond lengths are given in Ångström.

degree of bending in $CHT^{\bullet+}$ is less pronounced than in its neutral counterpart.[31] This is best illustrated by the values of the angles α and β displayed in Fig. 1 which are, respectively, 15.3° and 8.1° in $CHT^{\bullet+}$ compared to 57.2° and 27.7° in neutral[31] CHT, as optimized at the MP2/6–31G(d) level. The planar $CHT^{\bullet+}$ conformation obtained with MP2 is found to be a transition structure for inversion between two bent conformations of $CHT^{\bullet+}$. However, both a PMP2 barrier of 0.2 kcal mol^{-1} and an imaginary frequency of 54i cm^{-1} indicate that the PES is very flat in this region. The fact that, for both the geometry and the hyperfine structure of $CHT^{\bullet+}$, MP2 gives results which are in contradiction with those of most theoretical and experimental investigations strongly suggests that the bent geometry found by MP2 for this cation is only an artefact of this computational method. However, the low energy required for inverting the MP2 structure may indicate that the measured ^1H hfcc values may be average values over the reaction path between two bent structures, which proceeds through a planar transition structure. It should be noted that, very recently, similar unexpected results have been found for benzene and some other planar arenes, at MP2, MP3, CISD and CCSD levels in combination with a number of popular basis sets.[34]

Isomerization pathways from $N^{\bullet+}$ to $CHT^{\bullet+}$

Gibbs energy profiles for the three isomerization mechanisms from $N^{\bullet+}$ to $CHT^{\bullet+}$ investigated in the present study, are displayed in Fig. 3. For all stationary points, the relative electronic energies are reported in Table 2 together with Gibbs energies.

An investigation of the vibrational normal modes of $N^{\bullet+}$ shows that it has four low frequencies (377, 385, 395 and 460 cm^{-1}). The

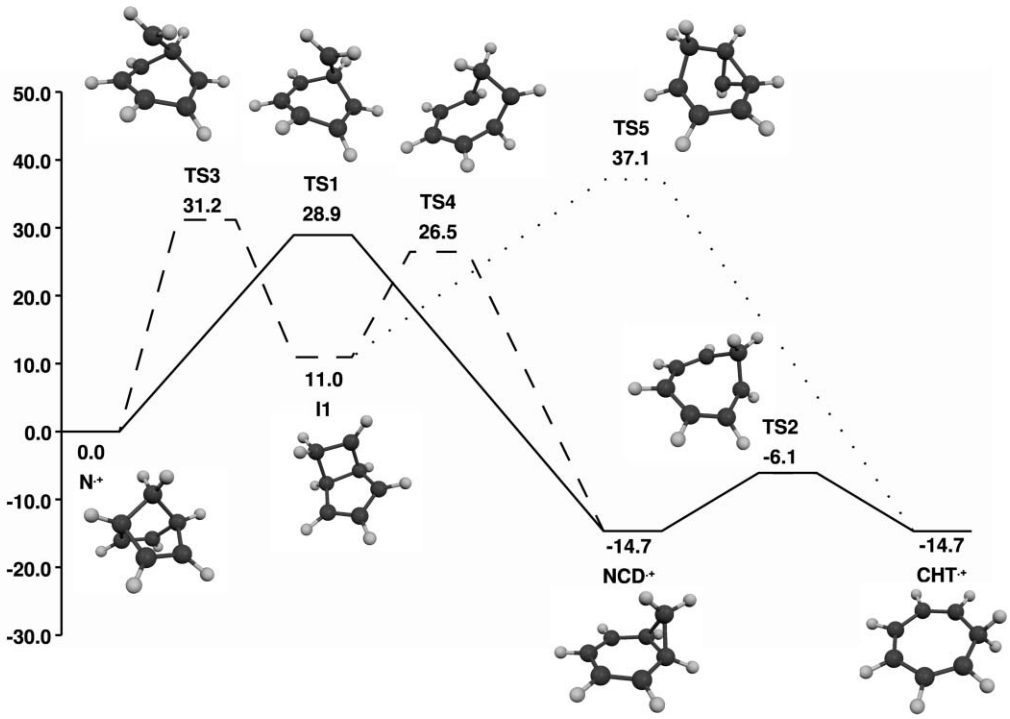

Fig. 3 Gibbs energy profiles (in kcal mol^{-1}) computed from CCSD(T)/6–311+G(d,p) electronic energies and B3LYP/6–311+G(d,p) thermal corrections to Gibbs free energy at 100.0 K and 1.0 atm for the three isomerization reactions from $N^{\bullet+}$ to $CHT^{\bullet+}$ investigated in the present study.

Table 2 Relative electronic energies and Gibbs energies (in kcal mol^{-1}) for all stationary points involved in the three isomerization pathways from $N^{\bullet+}$ to $CHT^{\bullet+}$

	B3LYP[a]	MP2[a]	PMP2[a]	CCSD(T)//B3LYP[a]	Gibbs energy[b]
$N^{\bullet+}$	0.0	0.0	0.0	0.0	0.0
$NCD^{\bullet+}$	−21.9	−9.6	−12.5	−14.2	−14.7
$CHT^{\bullet+}$	−28.9	−0.8	−8.4	−14.2	−14.7
I1	7.7	17.7	13.8	12.6	11.0
TS1	26.8	49.8[c]	38.2[c]	31.4	28.9
TS2	−12.8	4.9	−0.2	−4.7	−6.1
TS3	31.9	44.8[c]	37.7[c]	33.5	31.2
TS4	25.0	43.3	35.9	29.3	26.5
TS5	34.5	49.1	43.4	39.7	37.1

[a] The electronic energies are computed with B3LYP/6–311+G(d,p), MP2/6–311+G(d,p), PMP2/6–311+G(d,p) and CCSD(T)/6–311+G(d,p)//B3LYP/6–311+G(d,p). [b] The Gibbs energy includes the electronic CCSD(T)/6–311+G(d,p) energy as well as the zero-point vibrational energy and the thermal correction to Gibbs free energy computed with B3LYP/6–311+G(d,p) using the unscaled vibrational frequencies at 1.0 atm and 100 K. [c] Single point MP2/6–311+G(d,p) calculation on the HF/6–311+G(d,p) geometry.

normal mode of 385 cm^{-1}, for example, deforms the structure towards the pseudo-Jahn–Teller distorted transition structure between $N^{\bullet+}$ and $Q^{\bullet+}$ described previously[9,16]; and the 395 cm^{-1} mode describes the C_{2v} symmetric motion towards the conical intersection.[9] The normal modes responsible for cleavage of the bridgehead-methylene bonds, *i.e.* the motions toward TS1 and TS3, are found to lie much higher in the vibrational frequency spectrum (803, 904, 955 and 1008 cm^{-1}). This is entirely consistent with the relatively high activation energies of TS1 and TS3, 28.9 and 31.2 kcal mol^{-1}, respectively, compared to the activation energy of 17.9 kcal mol^{-1} found[16] for the formation of $Q^{\bullet+}$.

Concerted rearrangement to $NCD^{\bullet+}$: $N^{\bullet+}$ – TS1 – $NCD^{\bullet+}$

The first step of the lowest energy path to $CHT^{\bullet+}$ (solid line in Fig. 3) is a concerted transformation to $NCD^{\bullet+}$ *via* TS1 with an activation energy of 28.9 kcal mol^{-1}. This reaction is exothermic (−14.7 kcal mol^{-1}) and proceeds by asynchronous opening of the C_1–C_5 bond, rotation of the methylene group and formation of the C_1–C_7 bond. The major geometrical changes in the C_s symmetric transformation of $N^{\bullet+}$ to TS1 are the elongation of C_1–C_5 (from 1.552 to 2.366 Å) combined with a flattening of the cyclohexane ring and a shortening of the C_4–C_5 and C_5–C_6 bonds (from 1.525 to 1.453 Å). The imaginary vibrational frequency of TS1, 263i cm^{-1}, corresponds to the expected C_s symmetric opening and closure of the C_1–C_5 bond. The smallest of the four lowest real frequencies of TS1 (271, 413, 424 and 450 cm^{-1}) corresponds to CH_2 motion towards either C_4 or C_6, *i.e.*, towards a structure similar to TS3.

The formation of $NCD^{\bullet+}$, directly from TS1, was unexpected. In an experimental investigation[22] of the thermal rearrangement of N to CHT it was suggested that N most likely rearranges by opening of one of the bridgehead-methylene bonds to a diradical isotoluene intermediate (D), with one of the methyl hydrogens located at the *ipso*-position on the ring, before ring-closure to NCD. On the radical cation PES, D would correspond to a distonic species, $D^{\bullet+}$, which has been found to be a stable intermediate on the $C_7H_8^{\bullet+}$ PES at a variety of computational levels.[35–37] Also, a distonic metastable intermediate has been postulated for a fragmentation route of ionized 1-amino-7,7-dimethylnorbornan-2-ols which proceeds with initial cleavage of the bridgehead-methylene bond.[23] The IRC calculation starting from TS1 clearly shows that the opening of the bridgehead-methylene bond breaks symmetry before the distonic structure is formed. That is, at C_1–C_5 = ~3.8 Å, TS1 is twisted out of symmetry by a rotational motion of the CH_2 group, together with a shortening of the C_1–C_7 distance, until the lateral bond C_1–C_7 in the cyclopropane moiety is formed (see Fig. 1 for the atom labels).

In a constrained steepest descent optimization from TS1, where an approximate C_s symmetry is enforced for the bond opening by describing C_5–H_{1a} and C_5–H_{1b} by the same parameter, the formation of the distonic radical cation is found to be barrierless. In Fig. 4, the energies of the converged IRC (solid line) and constrained optimization (dashed line), relative to $NCD^{\bullet+}$, are plotted against the C_1–C_5 distance. This result suggests the existence of a branching point on the IRC, which separates the continued formation of the distonic ion from the formation of $NCD^{\bullet+}$. It can also be seen from inspection of Fig. 4 that even though the C_s symmetric formation of the distonic ion has no barrier beyond the branching region, it involves only a minor lowering of the energy, while the corresponding formation of $NCD^{\bullet+}$ is highly exothermic. It should also be noted that the rotation of the CH_2 group and the closure of the C_1–C_7 bond are the major reaction coordinates in the last part of the IRC-calculation.

We have also investigated the neutral transformation of N to NCD which was suggested to proceed *via* the diradical D in an experimental study.[22] Also in this case, we only locate a concerted pathway between N and NCD on the neutral singlet PES, at

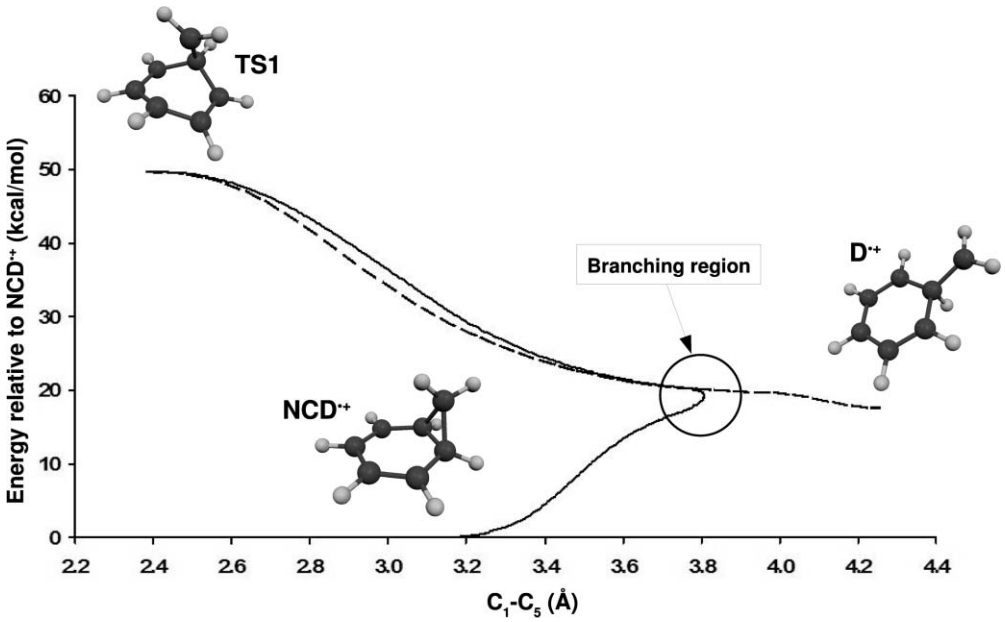

Fig. 4 The IRC calculation from TS1 to $NCD^{\bullet+}$ (solid line) and the constrained optimization scan from TS1 where approximate C_s symmetry is enforced for the C_1–C_5 bond opening (dashed line), as a function of the C_1–C_5 distance. Both calculations are performed at the B3LYP/6–31G(d,p) level of theory. The energy of $NCD^{\bullet+}$ is taken as zero.

the B3LYP/6–311+G(d,p) level. This path is therefore similar to the concerted $N^{\bullet+}$ – TS1 – $NCD^{\bullet+}$ rearrangement of the radical cation PES and the suggested[22] rearrangement *via* diradical D is probably not the minimum reaction path for transformation of neutral N to NCD. The geometry of the neutral concerted transition structure is found to be twisted out of symmetry. This can clearly be noticed by unequal C_1–C_4 and C_1–C_6 distances (2.676 and 2.883 Å, respectively) and H_{1a}–C_5 and H_{1b}–C_5 distances (2.609 and 3.579 Å, respectively). Since the corresponding C–C and H–C distances in radical cation TS1 are essentially equal (see Fig. 2), the neutral TS is in this respect an earlier transition structure for the concerted isomerization. Also note that the B3LYP/6–311+G(d,p) activation energy of the neutral concerted rearrangement to NCD is 52.6 kcal mol^{-1}, which is almost twice the barrier of the radical cation conversion (see Table 2). This result is entirely consistent with the fact that ionization of neutral compounds often results in substantial lowering of the energy barriers for isomerization reactions.

Stepwise rearrangement to $NCD^{\bullet+}$: $N^{\bullet+}$ – TS3 – I1 – TS4 – $NCD^{\bullet+}$

The second lowest energy path for isomerization of $N^{\bullet+}$ to $CHT^{\bullet+}$ located in the present work involves a stepwise conversion to $NCD^{\bullet+}$ (dashed line in Fig. 3). The first step is an endothermic (11.0 kcal mol^{-1}) transformation of $N^{\bullet+}$ to I1 *via* the rate-determining TS3, the activation energy of which is 31.2 kcal mol^{-1}. This is only 2.3 kcal mol^{-1} above TS1, which indicates that the stepwise channel is competitive with the concerted path.

The $N^{\bullet+}$ to I1 conversion involves breaking two bonds (C_1–C_5 and C_2–C_7) and forming two new bonds (C_1–C_4 and C_3–C_7). In the progression from $N^{\bullet+}$ to TS3, the major geometrical changes are opening of C_1–C_5 (from 1.553 to 2.163 Å) and a symmetry breaking motion of the CH_2 group towards C_4. This is reflected by the fact that, in TS3, the CH_2 group is closer to C_4 than to C_5, that is, C_1–C_4 = 2.024 and C_1–C_5 = 2.163 Å. The imaginary mode of TS3 (410i cm^{-1}) further reflects these asymmetric changes in the C_1–C_5 and C_1–C_4 bonds. In the reaction path from TS3 to I1, the formation of the C_3–C_7 bond (from 2.469 Å in TS3 to 1.564 Å in I1) and of the weak C_1–C_4 bond (from 2.024 to 1.613 Å) takes place before C_2–C_7 is broken (from 1.525 to 2.222 Å). Hence, the rearrangement of $N^{\bullet+}$ to I1 takes place through a complex reaction coordinate, first dominated by the cleavage of the C_1–C_5 bond before TS3 is formed, followed by the formation of the C_3–C_7 and C_1–C_4 bonds which takes place after TS3 is formed and, finally, the C_2–C_7 bond breaks.

The intermediate radical cation I1, which is displayed in Fig. 1, has structural similarities[15,16] with $BHD^{\bullet+}$. Both I1 and $BHD^{\bullet+}$ can be characterized as being composed of merged four-membered and five-membered ring moieties but the major difference between them is the position of the methylene carbon which is C_1 in I1 and C_7 in $BHD^{\bullet+}$. Also, the C_1–C_4 distance is 1.613 Å in I1, which corresponds to a very weak bond, compared[15,16] to 1.45 Å in $BHD^{\bullet+}$. On the other hand, the two double bonds of $BHD^{\bullet+}$ are located on separate ring fragments, prohibiting conjugation, whereas the fact that I1 is found to be 1.8 kcal mol^{-1} more stable than $BHD^{\bullet+}$ is most likely due to the effect of conjugation over C_5, C_6 and C_7 in I1, which is reflected by the lengths of C_5–C_6 (1.383 Å) and C_6–C_7 (1.397 Å) bonds of I1 in Fig. 1.

The highly exothermic (−25.6 kcal mol^{-1}) second step in the stepwise path to $NCD^{\bullet+}$ is the isomerization of I1 to $NCD^{\bullet+}$ *via* TS4 with an activation energy of 15.5 kcal mol^{-1}, as can be seen in Fig. 3. This rearrangement involves breaking the C_3–C_4 bond and forming a bond between C_2 and C_4 in I1. The reaction path from I1 to TS4 consists mainly in the elongation of C_3–C_4 from 1.564 to 1.764 Å, while on the path from TS4 to $NCD^{\bullet+}$ the reaction becomes a combination of continued elongation of this bond from 1.764 to 2.530 Å and the formation of the C_2–C_4 bond (from 2.033 Å in TS4 to 1.524 Å in $NCD^{\bullet+}$). It is found, by inspection of the vibrational frequencies of TS4, that the imaginary normal mode (583i cm^{-1}) corresponds to the combined asymmetric opening and closure of C_3–C_4 and C_2–C_4 which describes the major reaction coordinate between I1 and $NCD^{\bullet+}$.

Ring opening of $NCD^{\bullet+}$ to $CHT^{\bullet+}$: $NCD^{\bullet+}$ – TS2 – $CHT^{\bullet+}$

The opening of the cyclopropane ring of $NCD^{\bullet+}$, leading to $CHT^{\bullet+}$, proceeds *via* TS2 with an activation energy of 8.6 kcal mol^{-1} (see Fig. 3). This energy is slightly higher than the earlier theoretical estimates of 5–8 kcal mol^{-1}.[35–37] Moreover, in contrast to the previous computational studies[35–37] where $CHT^{\bullet+}$ was predicted to be 6–17 kcal mol^{-1} more stable than $NCD^{\bullet+}$, it is here found that both species have the same energy. Comparing the relative electronic energies of these species, the MP2 method predicts $NCD^{\bullet+}$ to be 8.8 kcal mol^{-1} more stable than $CHT^{\bullet+}$ (Table 2). This difference becomes lower with the spin-projected MP2, but $NCD^{\bullet+}$ is still 4.2 kcal mol^{-1} more stable than $CHT^{\bullet+}$ at this level. Again, this is probably a consequence of the severe spin-contamination of the MP2 wave-function for $CHT^{\bullet+}$. However, the situation is reversed at the B3LYP level, where $CHT^{\bullet+}$ is the most stable species by 7.0 kcal mol^{-1}, while CCSD(T) yields the same electronic energy for the two compounds. Thus the fact that our best computational estimate gives that $NCD^{\bullet+}$ has the same energy as $CHT^{\bullet+}$, and recalling that the activation energy for their inter-conversion is lower than the readily observable[5,7,12] isomerization of $Q^{\bullet+}$ to $N^{\bullet+}$ at the same level of theory (10.1 kcal mol^{-1}[16]), indicates that $NCD^{\bullet+}$ (Table 1) might be observable in ESR or ENDOR investigations of $CHT^{\bullet+}$. The geometrical changes between $NCD^{\bullet+}$ and $CHT^{\bullet+}$ found in the present study are consistent with those reported in the MINDO/3 study.[35] That is, the ring opening passes through an unsymmetric transition structure, and the imaginary normal mode (335i cm^{-1}) describes the opening and closing of C_2–C_7.

Rearrangement of I1 to $CHT^{\bullet+}$: I1 – TS5 – $CHT^{\bullet+}$

In addition to the two $N^{\bullet+}$ to $CHT^{\bullet+}$ reaction paths described above, which both proceed *via* $NCD^{\bullet+}$, we have also located a path which proceeds from I1 and directly to $CHT^{\bullet+}$. This third isomerization pathway is illustrated in Fig. 3 (see also Table 2). This rearrangement involves an exothermic (−25.6 kcal mol^{-1}) conversion *via* TS5 (Fig. 2) with an energy barrier of 26.2 kcal mol^{-1}. A major reaction coordinate is the elongation of the C_3–C_4 distance, from 1.564 Å in I1 to 2.205 Å in TS5 and further to 3.192 Å in $CHT^{\bullet+}$, together with a flattening of the carbon skeleton in $CHT^{\bullet+}$. Another important reaction coordinate is the shortening/elongation of the C_2–C_7 distance, which decreases

from 2.222 Å in I1 to 1.614 Å in TS5 and it thereafter increases to 2.209 Å in $CHT^{\bullet+}$. From a detailed analysis of the I1 to TS5 conversion it can be noted that the formation of the C_2–C_7 bond takes place prior to the C_3–C_4 elongation. Thus, the elongation of C_3–C_4 is the dominating reaction coordinate, but the successive shortening and elongation of C_2–C_7 present also critical aspects of this reaction path.

Comparison of paths converting $N^{\bullet+}$ to $CHT^{\bullet+}$

A total of nine different channels for $N^{\bullet+}$ to $CHT^{\bullet+}$ conversion have been found and characterized with Gibbs energies at 100 K. In the present work three isomerizations, all initialized by opening of one bridgehead-methylene bond in $N^{\bullet+}$, have been reported. These are, a path involving a concerted rearrangement to $NCD^{\bullet+}$ ($N^{\bullet+}$ – $NCD^{\bullet+}$ – $CHT^{\bullet+}$) which is found to have the lowest activation energy, 28.9 kcal mol^{-1}; a mechanism with a stepwise isomerization to $NCD^{\bullet+}$ ($N^{\bullet+}$ – I1 – $NCD^{\bullet+}$ – $CHT^{\bullet+}$) which is 2.3 kcal mol^{-1} higher; and *via* a rearrangement of I1 directly to $CHT^{\bullet+}$ ($N^{\bullet+}$ – I1 – $CHT^{\bullet+}$) with the highest activation energy 8.2 kcal mol^{-1} above that of the lowest energy path. In an earlier publication, six multi-step paths were presented,[16] of which the most advantageous[15,16] involves an initial isomerization to $BHE^{\bullet+}$ *via* $Q^{\bullet+}$ thereafter followed by a multi-step rearrangement to $CHT^{\bullet+}$. An activation energy of 24.3 kcal mol^{-1} was found for this path, which is 4.6 kcal mol^{-1} lower than the path *via* a concerted isomerization to $NCD^{\bullet+}$ of the present study. Thus, the multi-step rearrangement channel found previously[16] is the lowest energy path characterized for the $N^{\bullet+}$ to $CHT^{\bullet+}$ isomerization.

Comparison of the electronic energies relative to $N^{\bullet+}$

As seen in Table 2, the stability of the stationary points very much depends on the theoretical method used in the computation. Using our best computational method, CCSD(T), as a benchmark, clear trends can be noted in the B3LYP, MP2 and PMP2 electronic energies. First, it is found that B3LYP underestimates the energy of all structures relative to $N^{\bullet+}$. Compared to the CCSD(T) calculations, this over-stabilization ranges from −1.6 kcal mol^{-1} for TS3 to −14.7 kcal mol^{-1} for $CHT^{\bullet+}$ (see Table 2), hence reproducing the result[16] reported earlier for $CHT^{\bullet+}$. For MP2 the opposite is found. Hence, the unprojected MP2 method overestimates the energies relative to $N^{\bullet+}$ from 4.6 kcal mol^{-1} for $NCD^{\bullet+}$ to 18.4 kcal mol^{-1} for TS1. An improvement is noted when using projected MP2, as can be seen in Table 2, but the PMP2 energies are still too large, ranging from 1.7 kcal mol^{-1} for $NCD^{\bullet+}$ to 6.8 kcal mol^{-1} for TS1, compared with the relative energies predicted by CCSD(T).

Substitution effects on the concerted pathway

In recent experiments it was observed[23] that cleavage of the bridgehead-methylene bond becomes favoured over other paths for ionized 1-amino-7,7-dimethylnorbornan-2-ols while for the isomeric 1-amino-3,3-dimethylnorbornan-2-ols it is not observed. This result led us to investigate the effects of substitution on the concerted isomerization channel to $NCD^{\bullet+}$. Of particular interest is to investigate whether the concerted channel leading to $CHT^{\bullet+}$ can become competitive with the multi-step minimum energy path presented previously[16] after such substitutions.

We have therefore performed a study of the concerted and multi-step paths where H1a and H1b (see Fig. 1) are substituted with two methyl groups. The names of the stationary structures which are involved in the multi-step path have been taken from the previous article[16] but are (except for $Q^{\bullet+}$ and $BHE^{\bullet+}$) augmented with the prefix "MS-". All substituted species are given the suffix "-$2CH_3$". Thus, the substituted reaction sequence of the multi-step path[16] becomes N-$2CH_3^{\bullet+}$ – MS-TS1-$2CH_3$ – Q-$2CH_3^{\bullet+}$ – MS-TS2-$2CH_3$ – BHE-$2CH_3^{\bullet+}$ – MS-TS6-$2CH_3$ – MS-I1-$2CH_3$ – MS-TS7-$2CH_3$ – MS-I2-$2CH_3$ – MS-TS9-$2CH_3$ – CHT-$2CH_3^{\bullet+}$, while the substituted reaction sequence of the concerted channel is N-$2CH_3^{\bullet+}$ – TS1-$2CH_3$ – NCD-$2CH_3^{\bullet+}$ – TS2-$2CH_3$ – CHT-$2CH_3^{\bullet+}$.

A comparison of the geometries for the substituted and unsubstituted minima shows that the bonds connected to the substituted methylene carbon are involved in the largest changes. Typically these bonds are enlarged by 0.01–0.02 Å upon substitution while the other C–C bonds deviate by less than 0.01 Å. However, larger deviations are found in N-$2CH_3^{\bullet+}$ and NCD-$2CH_3^{\bullet+}$. In N-$2CH_3^{\bullet+}$, the C_1–C_2 and C_1–C_5 bonds (see Fig. 1 for the labels) are found to be 0.030 Å longer than in $N^{\bullet+}$, indicating a substantial weakening of the bridgehead-methylene bonds in the substituted norbornadiene radical cation. It is also interesting to note that, upon substitution, the lateral C_1–C_2 and C_1–C_7 bonds in the cyclopropane moiety of $NCD^{\bullet+}$ increase from 1.543 to 1.602 and 1.593 Å, respectively, while the internal C_2–C_7 bond decreases from 1.524 to 1.502 Å. This has two consequences; first, the C_S symmetry is broken in the substituted norcaradiene radical cation and, second, the cyclopropane moiety in NCD-$2CH_3^{\bullet+}$ has a structure corresponding to the $^2B_2$ electronic state (one short and two long bonds) of the cyclopropane radical cation, which is the higher energy product when cyclopropane undergoes Jahn–Teller distortion upon ionization.[30]

The structural changes induced by the substitution on the transition structures involved in the multi-step path follow the same trend as the minima. That is, the C–C bonds connected with the substituted methylene carbon atom generally account for the largest differences, increasing by 0.01–0.02 Å. A larger difference is, however, found in the breaking C–C bond in MS-TS9-$2CH_3$ which is enlongated by 0.067 Å, compared to MS-TS9, which hence yields a later transition structure for the final step in the multi-step path compared with the unsubstituted case.

The geometry of the transition structure for cleavage of the bridgehead-methylene bond in the concerted path is substantially affected by the added methyl groups. The structure of TS1-$2CH_3$ is displayed in Fig. 5 together with selected geometrical parameters. An inspection of the figure reveals that the breaking C_1–C_5 bond distance decreases by 0.357 Å compared to TS1 (see Fig. 1 and 5). Moreover, while TS1 is a C_S symmetric transition structure for the unsubstituted reaction, the bond distances in TS1-$2CH_3$ (Fig. 5) clearly show that the symmetry is broken in the substituted case. This symmetry breaking can be further confirmed by the unequal C_5–C_8 and C_5–C_9 distances of 2.983 and 2.817 Å, respectively, in TS1-$2CH_3$ (Fig. 5). This shows that the methylene group is twisted out of symmetry, similar to the neutral transition structure between N and NCD. Thus, the transition structure between the substituted norbornadiene and norcaradiene radical cations is much earlier than the corresponding unsubstituted transition structure.

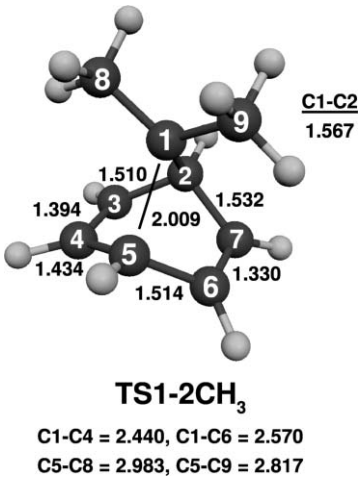

Fig. 5 B3LYP/6–311+G(d,p) optimized geometry of the transition structure between the substituted norbornadiene and norcaradiene radical cations. Bond lengths are given in Ångström.

Fig. 6 (Fig. 7) displays energy profiles for both the concerted and multi-step unsubstituted (substituted) pathways. An inspection of these figures shows that the multi-step isomerization is hardly affected at all energetically by the substitution. The largest impact is found for MS-TS1, which is lowered by 1.4 kcal mol^{-1} by the addition of the methyl groups. The rate-determining transition structure of the multi-step path (MS-TS2, 24.2 kcal mol^{-1}, see Fig. 6) does still remain the point of highest energy after substitution (MS-TS2-2CH$_3$, 23.8 kcal mol^{-1}, see Fig. 7). For the concerted path on the contrary, the energy profiles (Fig. 6 and 7) reveal that the substitution has a large stabilizing effect on TS1. That is, the transition structure for cleavage of the bridgehead-methylene bond is lowered from 26.7 kcal mol^{-1} in TS1 to 18.2 kcal mol^{-1} in TS1-2CH$_3$. As a consequence, while the rate-determining TS1 is 2.5 kcal mol^{-1} higher than MS-TS2 (see Fig. 6), the substitution makes this order reversed as the corresponding TS1-2CH$_3$ is 5.6 kcal mol^{-1} lower than MS-TS2-2CH$_3$ which becomes then the point of highest energy on the substituted profiles (see Fig. 7). Indeed, this result is in accordance with the experimental observation[23] that a substitution of this type favours bridgehead-methylene bond breaking in ionized 1-amino-7,7-dimethylnorbornan-2-ols. Yet, the stabilization of the concerted path is dramatic (8.5 kcal mol^{-1}), and this channel thus becomes the dominating pathway for the transformation of the substituted norbornadiene radical cation to cycloheptatriene.

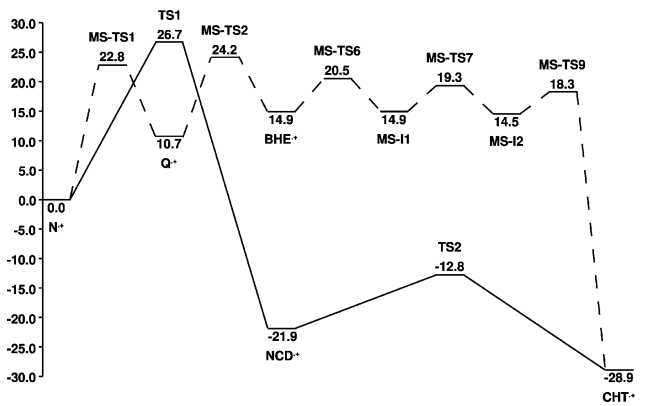

Fig. 6 B3LYP/6–311+G(d,p) energy profiles (in kcal mol^{-1}) for the concerted (solid line) and the multi-step[16] (dashed line) pathways from N$^{\bullet+}$ to CHT$^{\bullet+}$.

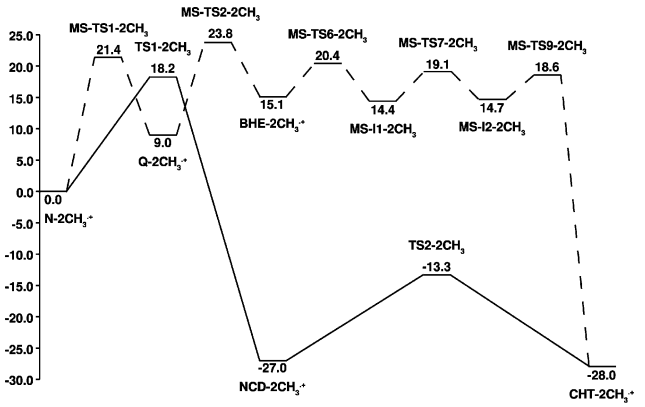

Fig. 7 B3LYP/6–311+G(d,p) energy profiles (in kcal mol^{-1}) for the concerted (solid line) and the multi-step[16] (dashed line) pathways from substituted N$^{\bullet+}$ to CHT$^{\bullet+}$.

Conclusions

Three skeletal rearrangement pathways from N$^{\bullet+}$ to CHT$^{\bullet+}$, by opening of one bridgehead-methylene bond in N$^{\bullet+}$, have been located in the present work. The most favorable path is described by a concerted formation of NCD$^{\bullet+}$ followed by ring opening to CHT$^{\bullet+}$. This low-energy path proceeds with an activation energy of 28.9 kcal mol^{-1}, which is 4.6 kcal mol^{-1} higher than the barrier for the multi-step path from N$^{\bullet+}$ to CHT$^{\bullet+}$ *via* BHE$^{\bullet+}$ reported previously.[16] Interestingly, when the two hydrogen atoms in the methylene group are substituted against methyl groups the barrier for the concerted channel is lowered by 8.5 kcal mol^{-1} at the B3LYP/6–311+G(d,p) level of theory. This large stabilization is accompanied by a substantial change in the geometry of the rate-determining transition structure. The same substitution has only a modest impact on the energetics of the multi-step path and the overall barrier for this channel is found to be 5.6 kcal mol^{-1} higher than for the concerted pathway. Hence, in the substituted system, the concerted channel is the most favourable pathway for the isomerization of the norbornadiene radical cation to cycloheptatriene.

No distonic iso-toluene radical cation intermediate is found along the path between N$^{\bullet+}$ and NCD$^{\bullet+}$. Instead it is found that after the formation of TS1, a branching point is distorting the IRC away from C_s symmetry, which would otherwise lead to the formation of iso-toluene. For the corresponding neutral rearrangement of N to CHT, a concerted rearrangement to NCD is located with an activation energy of 52.6 kcal mol^{-1} at the B3LYP/6–311+G(d,p) level. Thus, no transition structure connecting to the suggested[22] diradical intermediate is found in the present study, and as a result neither the radical cation nor the neutral conversion proceeds *via* the iso-toluene intermediate.

Besides the characterization of different reaction pathways, there are also in the present study three results concerning NCD$^{\bullet+}$ and CHT$^{\bullet+}$ which are worth emphasizing. First, NCD$^{\bullet+}$ and CHT$^{\bullet+}$ are predicted to have identical energies, in contradiction

with the computations of earlier theoretical investigations[35–37] where $CHT^{\bullet+}$ was found to be 6–17 kcal mol^{-1} more stable than $NCD^{\bullet+}$. Second, the activation energy for their interconversion (8.6 kcal mol^{-1}) is computed to be 1.5 kcal mol^{-1} lower[16] than that of the facile isomerization[5,7,12] of $Q^{\bullet+}$ to $N^{\bullet+}$. These two results indicate that $NCD^{\bullet+}$ might be detected in ESR measurements of $CHT^{\bullet+}$. Third, in contradiction to earlier theoretical,[16,31] and most experimental,[5,29,32] results as well as with the present B3LYP/6–311+G(d,p) calculation, $CHT^{\bullet+}$ is optimized with MP2/6–311+G(d,p) to a bent structure. This is a structure that is similar to neutral[31] CHT, but with a more planar geometry. Moreover, the barrier for inversion through the planar conformation is only 0.2 kcal mol^{-1}.

Acknowledgements

A Marie Curie Intra European Fellowships supported the work of PEL-contract No MEIF-CT-2004-501535. "The authors are solely responsible for the information communicated and it does not represent the opinion of the European Community. The European Community is not responsible for any use that might be made of data appearing therein". We thank the Swedish National Supercomputer Center (NSC) for generous allocation of computer time. The authors are indebted to Prof. S. Lunell and Prof. O. Matsson for helpful discussions.

References

1 H. D. Roth, *Adv. Theor. Interesting Mol.*, 1995, **3**, 261–302.
2 See, *e.g.*, M. V. Barnabas and A. D. Trifunac, *J. Chem. Soc., Chem. Commun.*, 1993, **10**, 813–814.
3 H. D. Roth, M. L. M. Schilling and G. Jones, *J. Am. Chem. Soc.*, 1981, **103**, 1246–1248.
4 K. Raghavachari, R. C. Haddon and H. D. Roth, *J. Am. Chem. Soc.*, 1983, **105**, 3110–3114.
5 G.-F. Chen, J. T. Wang, F. Williams, K. D. Belfield and J. E. Baldwin, *J. Am. Chem. Soc.*, 1991, **113**, 9853–9855.
6 K. Ishiguro, I. V. Khudyakov, P. F. McGarry, N. F. Turro and H. D. Roth, *J. Am. Chem. Soc.*, 1994, **116**, 6933–6934.
7 K. R. Cromack, D. W. Werst, M. V. Barnabas and A. D. Trifunac, *Chem. Phys. Lett.*, 1994, **218**, 485–491.
8 R. D. Bach, I. L. Schilke and H. B. Schlegel, *J. Org. Chem.*, 1996, **61**, 4845–4847.
9 T. Clark, *Acta Chem. Scand.*, 1997, **57**, 646–652.
10 Y. Inadomi, K. Morihasi and O. Kikuchi, *J. Mol. Struct.*, 1998, **434**, 59–66.
11 P. G. Gassman and J. W. Hershberger, *J. Org. Chem.*, 1987, **52**, 1337–1339.
12 M. V. Barnabas, D. W. Werst and A. D. Trifunac, *Chem. Phys. Lett.*, 1993, **206**, 21–24.
13 W. Adam, T. Heidenfelder and C. Sahin, *J. Am. Chem. Soc.*, 1995, **117**, 9693–9698.
14 R. E. Bühler and M. A. Quadir, *J. Phys. Chem. A*, 2000, **104**, 2634–2640.
15 P.-E. Larsson, N. Salhi-Benachenhou, X.-C. Dong and S. Lunell, *Int. J. Quantum Chem.*, 2002, **90**, 1388–1395.
16 P.-E. Larsson, N. Salhi-Benachenhou and S. Lunell, *Chem.–Eur. J.*, 2004, **10**, 681–688.
17 All abbreviations are explained in the Computational Details section.
18 P.-E. Larsson, N. Salhi-Benachenhou and S. Lunell, *Org. Lett.*, 2003, **5**, 1329–1331.
19 P.-E. Larsson and N. Salhi-Benachenhou, unpublished work.
20 R. Herges, F. Starck, T. Winkler and M. Schmittel, *Chem.–Eur. J.*, 1999, **5**, 2965–2970.
21 A. J. Jarzecki, J. Gajewski and E. R. Davidson, *J. Am. Chem. Soc.*, 1999, **121**, 6928–6935.
22 W. G. Woods, *J. Org. Chem.*, 1958, **23**, 110–112.
23 A. G. Martínez, E. T. Vilar, A. G. Fraile, R. Martínez-Álvarez, S. de la M. Cerero and P. Martínez-Ruiz, *Rapid Commun. Mass Spectrom.*, 2005, **19**, 1005–1010.
24 M. J. Frisch, G. W. Trucks, H. B. Schlegel, G. E. Scuseria, M. A. Robb, J. R. Cheeseman, J. A. Montgomery, Jr., T. Vreven, K. N. Kudin, J. C. Burant, J. M. Millam, S. S. Iyengar, J. Tomasi, V. Barone, B. Mennucci, M. Cossi, G. Scalmani, N. Rega, G. A. Petersson, H. Nakatsuji, M. Hada, M. Ehara, K. Toyota, R. Fukuda, J. Hasegawa, M. Ishida, T. Nakajima, Y. Honda, O. Kitao, H. Nakai, M. Klene, X. Li, J. E. Knox, H. P. Hratchian, J. B. Cross, V. Bakken, C. Adamo, J. Jaramillo, R. Gomperts, R. E. Stratmann, O. Yazyev, A. J. Austin, R. Cammi, C. Pomelli, J. Ochterski, P. Y. Ayala, K. Morokuma, G. A. Voth, P. Salvador, J. J. Dannenberg, V. G. Zakrzewski, S. Dapprich, A. D. Daniels, M. C. Strain, O. Farkas, D. K. Malick, A. D. Rabuck, K. Raghavachari, J. B. Foresman, J. V. Ortiz, Q. Cui, A. G. Baboul, S. Clifford, J. Cioslowski, B. B. Stefanov, G. Liu, A. Liashenko, P. Piskorz, I. Komaromi, R. L. Martin, D. J. Fox, T. Keith, M. A. Al-Laham, C. Y. Peng, A. Nanayakkara, M. Challacombe, P. M. W. Gill, B. G. Johnson, W. Chen, M. W. Wong, C. Gonzalez and J. A. Pople, *GAUSSIAN 03 (Revision C.02)*, Gaussian, Inc., Wallingford, CT, 2004.
25 P. Flükiger, H. P. Lüthi, S. Portmann and J. Weber, *MOLEKEL-4.3*, Swiss Center for Scientific Computing, Manno, Switzerland, 2000.
26 H. B. Schlegel, *J. Phys. Chem.*, 1988, **92**, 3075–3078.
27 R. Batra, B. Giese, M. Spichty, G. Gescheidt and K. N. Houk, *J. Phys. Chem.*, 1996, **100**, 18371–18379.
28 M. Alcamí, O. Mó and M. Yáñez, *Mass Spectrom. Rev.*, 2001, **20**, 195–245.
29 A. Faucitano, A. Buttafava and F. Martinotti, *Radiat. Phys. Chem.*, 1995, **45**, 45–49.
30 T. Herbertz, F. Blume and H. D. Roth, *J. Am. Chem. Soc.*, 1998, **120**, 4591–4599.
31 Y. Inadomi, K. Morihashi and O. Kikuchi, *THEOCHEM*, 1998, **428**, 143–148.
32 A. Faucitano, A. Buttafava, F. Martinotti, R. Sustmann and H.-G. Korth, *J. Chem. Soc., Perkin Trans. 2*, 1992, **6**, 865–869.
33 Y. Kubozono, T. Miyamoto, M. Aoyagi, M. Ata, Y. Matsuda, Y. Gondo, H. Nakamura and T. Matsuo, *Chem. Phys.*, 1992, **160**, 421–426.
34 D. Moran, A. C. Simmonett, F. E. Leach, III, W. D. Allen, P. v. R. Schleyer and H. F. Schaefer, III, *J. Am. Chem. Soc.*, 2006, **128**, 9342–9343.
35 M. J. S. Dewar and D. Landman, *J. Am. Chem. Soc.*, 1977, **99**, 2446–2453.
36 C. Lifshitz, Y. Gotkis, A. Ioffe, L. Laskin and S. Shaik, *Int. J. Mass Spectrom. Ion Processes*, 1993, **125**, R7–R11.
37 H.-F. Grützmacher and N. Harting, *Eur. J. Mass Spectrom.*, 2003, **9**, 327–341.

